Effective-medium method for hopping transport in a magnetic field

O. Bleibaum and H. Böttger
Institut für Theoretische Physik, Otto-von-Guericke-Univerisität Magdeburg, Universitätsplatz 2, PF 4120, 39016 Magdeburg, Germany

V. V. Bryksin
A. F. Ioffe Physico-Technical Institute, Politekhnicheskaya 26, 194021 St. Petersburg, Russia
(Received 25 November 1996; revised manuscript received 14 April 1997)

An effective-medium theory for studying the influence of a magnetic field on hopping transport has been developed. It permits both the magnetoconductivity and the Hall effect to be studied in the nearest-neighbor-hopping (NNH) and in the variable-range-hopping (VRH) regime. The method has been applied to the dc and ac Hall effect in three-dimensional systems. For NNH the static Hall mobility proves to be exponentially small in the critical hopping length. This fact results in a change of the sign of the Hall mobility of intermediate frequencies. For VRH the dc Hall mobility exhibits a powerlike dependence on temperature. Owing to this fact the Hall mobility is nearly independent of frequency for small frequencies. [S0163-1829(97)01935-8]

I. INTRODUCTION

During the past three decades the Hall effect in the hopping regime has been a point of controversy. The first who succeded in investigating the effect was Holstein.[1] Stressing the importance of the electron phonon interaction, he introduced a three-site model. The influence of the magnetic field on hopping transport was properly taken into account in the phase factors of the resonance integrals. Using his model he established a theory for the Hall effect in the high-frequency limit. Although his theory covers both nearest-neighboring hopping (NNH) and variable-range hopping (VRH) he restricted his calculations to the NNH regime, where he found the Hall mobility to be two orders of magnitude larger than the drift mobility.

Encouraged by this unexpected result, Amitay and Pollak[2] tried to verify Holstein's predictions experimentally. They found a serious discrepancy: the measured Hall voltage proved to be orders of magnitude smaller, as estimated by Holstein.

Since then, many articles have been devoted to the theory of the dc Hall effect (e.g., Refs. 3–12) by using different methods. While in the NNH regime the percolation theory and the effective medium method have proved particularly useful; in the VRH regime mainly the percolation theory has been applied. Unlike NNH, VRH is not only a problem of particle diffusion but also of energy diffusion, which makes it more difficult to treat analytically. The standard effective-medium theory proves to be inapplicable to the study of the conductivity in the VRH regime.[13,14] Refined effective-medium treatments have been published in Refs. 15–17. While in the effective-medium approach of Ref. 15 the disordered solid is modeled on a Cayley tree, the effective-medium approaches of Refs. 16 and 17 do not rely on the introduction of a reference lattice. To overcome the dependence on the lattice in Ref. 16, the diagrammatic technique by Gouchanour, Andersen, and Fayer[18] for the self-consistent calculation of the conditional probability function was used. In contrast to to Ref. 16, in Ref. 17 the configurational averaged conductivity was deduced from the long-distance behavior of the diffusion propagator, which comprises both particle and energy diffusion. To this end, a self-consistent framework for the calculation of the long-distance contribution to the diffusion propagator has been developed. However, apart from the effective-medium formalism of Ref. 15, no generalizations of these approaches to three-site correlations have been published so far.

For the NNH regime in all articles (e.g., Refs. 3–8) an exponential dependence of the Hall mobility on the critical hopping length was derived. For the VRH regime, the obtained results are controversal. The main point of controversy is related to the presence or absence of an exponential temperature dependence of the Hall mobility. A powerlike dependence of the Hall mobility on temperature was derived in Refs. 3, 5, and 9. In contrast, an exponential dependence of the Hall mobility on temperature was found in Refs. 10–12. The experimental data are considered as confirmation of an exponential temperature dependence of the Hall mobility (Refs. 19–23). However, comparing experimental and theoretical data one should keep in mind that the former are in general obtained close to the metal-insulator transition while the latter results were derived deep in the insulating regime.

The dependence of the Hall conductivity on frequency and on the magnetic field is still a less-investigated problem. In Ref. 24 the frequency dependence of the Hall conductivity in the NNH regime has been studied by means of the effective-medium method of Ref. 15. According to this calculation the Hall conductivity in the NNH exhibits qualitatively the same dependence on frequency as the longitudinal part of the conductivity. For small frequencies the authors of Ref. 24 obtain a powerlike dependence with respect to frequency. For high frequencies their result agrees with Holstein's result. For low and intermediate frequencies the real part of the Hall conductivity increases monotonously with increasing frequency. In the VRH regime a calculation of the frequency dependence of the Hall conductivity for small and intermediate frequencies has still been lacking. A calculation of the magnetic-field dependence of the Hall conductivity has not been published so far.

In this paper we present an effective-medium theory for

studying the influence of the magnetic field on hopping transport. The method is based on the effective-medium theory of Ref. 17. Beside the investigation of the exponential contribution to transport coefficients with respect to the critical hopping length, it permits also consideration of the preexponential factor. By means of our method we derive explicit equations for the symmetric part and for the antisymmetric part of the configurational averaged current with respect to the magnetic field. A further consideration of the symmetric part is, however, beyond the scope of the present paper. Using our theory we calculate the configurational averaged Hall conductivity both in the NNH and in the VRH regime. Doing so, we restrict our consideration to the strongly localized regime. We find that in this regime the Hall effect in the NNH regime differs from the Hall effect in the VRH regime in that different configurations give rise to the most relevant contributions to the Hall current. This fact leads to interesting differences between the behavior of the Hall conductivity in the NNH regime and the behavior of the Hall conductivity in the VRH regime in the presence of higher magnetic and alternating electric fields which have not been published in the literature so far. Our calculation shows that, in contrast to the VRH regime, where the linear situation with respect to the magnetic field is realized also for higher magnetic fields, the Hall conductivity in the NNH regime exhibits quantum oscillations in dependence of the magnetic field. The period of these oscilations is given by the normal flux quantum. The fact that different configurations contribute to the current is manifest also in the frequency dependence. Whereas in the NNH regime the Hall mobility proves to be strongly dependent on frequency, the Hall mobility in the VRH regime is independent of frequency at all for small and intermediate frequencies. The frequency dependence of the Hall conductivity in the NNH regime obtained by means of our method differs from that derived in Ref. 24. In contrast to Ref. 24, where the real part of the Hall conductivity increases monotonously for intermediate frequencies, our calculation predicts a change of sign of the effect. For small and high frequencies our results agree with those found in Ref. 24 and Ref. 1.

Although our main results have been derived deep in the strongly localized regime, our method itself is not restricted to that limit. Also, in those regimes where the most pronounced temperature dependence of the Hall mobility in the VRH regime is not governed by the powerlike dependence on the critical hopping length our method can be used to determine exponential prefactors. Instead of performing dc measurements by varying the temperature in a large range, we suggest ac measurements with fixed temperature.

II. BASIC EQUATIONS

For the calculation of the current we use the conditional probability function approach developed in Ref. 17. Within this approach the current is calculated from the Green's function $P_{m'm}$ according to

$$\mathbf{j}(s)=\frac{e^2s^2}{kT\Omega}\sum_{m'm}(\mathbf{R}_{m'}-\mathbf{R}_m)(\mathbf{E}\mathbf{R}_{m'})C_{m'}P_{m'm}(s). \quad (1)$$

Here $C_m=f_m(1-f_m)$, where $f_m=f(\epsilon_m)$ is the Fermi distribution function with site energy ϵ_m, $\mathbf{R}_m$ is the position vector of site m, Ω is the volume, $\mathbf{E}$ is the electric-field strength, and $s=-i\omega$, where ω is the frequency of the applied electric field. The Green's function $P_{m'm}$ satisfies the equation

$$sP_{m'm}=\delta_{m'm}+\sum_{m''}\Gamma_{m''m}\{C_{m''}^{-1}P_{m'm''}-C_m^{-1}P_{m'm}\}. \quad (2)$$

The quantities $\Gamma_{m'm}$ are related to the transition probabilities entering the rate equations in the absence of the electric field.[25] In the absence of a magnetic field their calculation may be restricted to two-site processes. In this case they are symmetric with respect to their indices. The study of the influence of a magnetic field requires us to go beyond this approximation and to include three-site processes in our consideration. In that case they can be decomposed into their two-site parts and into their three-site parts according to

$$\Gamma_{m'm}=\Gamma_{m'm}^{(2)}+\Gamma_{m'm}^{(3)}, \quad (3)$$

where the two-site part $\Gamma^{(2)}$ is independent of the field. The three-site part describes the interference of amplitudes of alternative hopping paths via a third site. Accordingly, it can be written in the form

$$\Gamma_{m'm}^{(3)}=\sum_{m_3}\Gamma_{m'm_3m}. \quad (4)$$

The quantities $\Gamma_{m_1m_2m_3}$ can be further decomposed into their symmetric and into their antisymmetric parts with respect to the external magnetic field. These parts obey the following relations of symmetry:

$$\Gamma_{m_1m_2m_3}^{(s)}=\Gamma_{m_3m_2m_1}^{(s)}, \quad (5)$$

$$\Gamma_{m_1m_2m_3}^{(a)}=-\Gamma_{m_3m_1m_2}^{(a)}=-\Gamma_{m_1m_3m_2}^{(a)}. \quad (6)$$

In the course of these relations the quantity $\Gamma_{m'm}$ satisfies the equation

$$\Gamma_{m'm}(\mathbf{H})=\Gamma_{mm'}(-\mathbf{H}). \quad (7)$$

Owing to the principle of detailed balance and the law of probability conservation the Green's function $P_{m'm}$ obeys the sum rules

$$s\sum_{m'}C_{m'}P_{m'm}=C_m, \quad (8)$$

$$s\sum_{m}P_{m'm}=1. \quad (9)$$

Both relations can be easily derived by means of Eq. (2).

Note that in the presence of a magnetic field it is not possible to rewrite Eq. (1) in such a way that it only involves the differences of the position vectors of the sites. Nevertheless, it is independent of the choice of the coordinate system, which is to be seen from an explicit displacement of the coordinate system and an application of the sum rules [Eqs. (8) and (9)].

To proceed further, a decomposition of all quantities into disordered quantities and disorder-independent ones proves

to be useful. This is achieved by changing the representation from discrete to continous coordinates. The transition is performed by defining the new Green's function,

$$P(\rho',\rho)=\sum_{m'm}\delta(\rho'-\rho_{m'})P_{m'm}\delta(\rho-\rho_m), \tag{10}$$

where $\rho_m=\{\mathbf{R}_m,\epsilon_m\},\rho=\{\mathbf{R},\epsilon\}$. In the new representation (10) expression (1) for the current takes the form

$$\mathbf{j}=\frac{e^2s^2}{kT\Omega}\int d\rho' d\rho(\mathbf{R}'-\mathbf{R})(\mathbf{E}\mathbf{R}')C(\epsilon')P(\rho',\rho). \tag{11}$$

Moreover, the equation of motion for the Green's function (2) may be cast into the form

$$sP(\rho',\rho)=\eta(\rho)\delta(\rho'-\rho)+\int d\rho''P(\rho',\rho'')V(\rho'',\rho), \tag{12}$$

where $\eta(\rho)=\Sigma_m\delta(\rho-\rho_m)$ is the structural factor. The potential V is given by

$$V(\rho',\rho)=\int d\rho''\eta(\rho'')C^{-1}(\epsilon')\{\Gamma(\rho',\rho'')\delta(\rho''-\rho) -\Gamma(\rho'',\rho')\delta(\rho'-\rho)\}, \tag{13}$$

where $\Gamma(\rho',\rho)=\Gamma_{m'm}|_{\rho_{m'}=\rho',\rho_m=\rho}$. Due to the decomposition (3) the potential V can be also decomposed into its two-site part and into its three-site parts. Its two-site approximation $V^{(2)}$ is determined by the structural factor η and by the function $\Gamma^{(2)}$. As $\Gamma^{(2)}$ is independent of the disorder, $V^{(2)}$ depends on disorder solely via the function η. The three-site part of the potential V is determined by the the structural factor η and the three-site contribution $\Gamma^{(3)}$. As the latter contribution is not only determined by the initial and the final site, but also by an intermediate third site, it is still affected by disorder. In fact, it can be written in the form

$$\Gamma^{(3)}(\rho',\rho)=\int d\rho_3\eta(\rho_3)\Gamma(\rho',\rho_3,\rho), \tag{14}$$

where $\Gamma(\rho',\rho_3,\rho)=\Gamma_{m'm_3m}|_{\rho_{m'}=\rho',\rho_{m_3}=\rho_3,\rho_m=\rho}$. Consequently, the the three-site part $V^{(3)}$ of the potential V contains two factors of the structural factor η.

Below, we focus on the calculation of the configuration-averaged conductivity. The solution of this problem requires the calculation of an approximate solution of Eq. (12) and the performance of the averaging procedure. For the two-site approximation this program has been performed in Ref. 17. In the presence of the magnetic field the solution of the problem is rendered more difficult by the fact that the potential V is nonlinear with respect to the structural factor η. However, an important simplification can be achieved by observing that $\Gamma^{(3)}\ll\Gamma^{(2)}$. Using the smallness of $\Gamma^{(3)}$ with respect to $\Gamma^{(2)}$ we linearize Eq. (12) with respect to the third site. Accordingly, we decompose P into its two-site part $P^{(2)}$ and into its three-site part $P^{(3)}$. We stress that this simplification does not rely on the strength of the magnetic field.

To calculate the three-site part $P^{(3)}$ we introduce the function Φ, which represents the two-site approximation of the Green's function of Eq. (12). It is given by the solution of the equation

$$s\Phi(\rho',\rho)=\delta(\rho'-\rho)+\int d\rho''\Phi(\rho',\rho'')V^{(2)}(\rho'',\rho). \tag{15}$$

Using Φ, the two-site part of the conditional probability function P is given by $P^{(2)}(\rho',\rho)=\eta(\rho')\Phi(\rho',\rho)$. Consequently, the three-site part of P reads

$$P^{(3)}(\rho',\rho)=\int d\rho_1 d\rho_2\eta(\rho')\Phi(\rho',\rho_1)V^{(3)}(\rho_1,\rho_2) \times\Phi(\rho_2,\rho). \tag{16}$$

To proceed further it is expedient to introduce the function $\tilde{\Phi}$, which is defined by the relation $C(\epsilon')\eta(\rho')\Phi(\rho',\rho)=\tilde{\Phi}(\rho',\rho)\eta(\rho)C(\epsilon)$. According to its definition, the function $\tilde{\Phi}$ satisfies the equation

$$s\tilde{\Phi}(\rho',\rho)=\delta(\rho'-\rho)+\int d\rho''\tilde{\Phi}(\rho',\rho'')\tilde{V}^{(2)}(\rho'',\rho), \tag{17}$$

where

$$\tilde{V}^{(2)}(\rho',\rho)=C^{-1}(\epsilon)\int d\rho''\eta(\rho'')\Gamma(\rho'',\rho) \times\{\delta(\rho''-\rho)-\delta(\rho'-\rho)\}. \tag{18}$$

The advantage of the introduction of the function $\tilde{\Phi}$ lies in the fact that it moves the structural factor η in front of Eq. (16) from outside to inside. This fact proves to be advantageous in the performance of the averaging procedure. By means of Eqs. (17) and (18) the magnetic-field dependent part of the current can be written in the form

$$\mathbf{j}_H=-\frac{e^2s^2}{kT\Omega}\int d\rho' d\rho d\rho_1 d\rho_2 d\rho_3\mathbf{R}(\mathbf{E}\mathbf{R}') \times\tilde{\Phi}(\rho',\rho_1)\eta(\rho_1)\eta(\rho_2)\eta(\rho_3)\{\Gamma(\rho_1,\rho_3,\rho_2)\Phi(\rho_2,\rho) -\Gamma(\rho_2,\rho_3,\rho_1)\Phi(\rho_1,\rho)\}. \tag{19}$$

In order to obtain Eq. (19) we have taken advantage of the symmetry relations (5) and (6).

III. CALCULATION OF THE CONFIGURATION-AVERAGED CURRENT

For the calculation of the configuration-averaged current density we use the configuration-averaging technique for the structural factor η proposed in Ref. 17. The technique implies a diagrammatic expansion of expression (19) in powers of the structural factor η and the subsequent application of the averaging procedure to the individual terms.

In order to expand Eq. (19) with respect to η we have to find a series expansion of the functions Φ and $\tilde{\Phi}$. Such an expansion can be obtained by reiterating Eq. (15) and Eq. (17), so that the series of the kernel of the current (19) can be represented as depicted in Fig. 1. To calculate the configu-

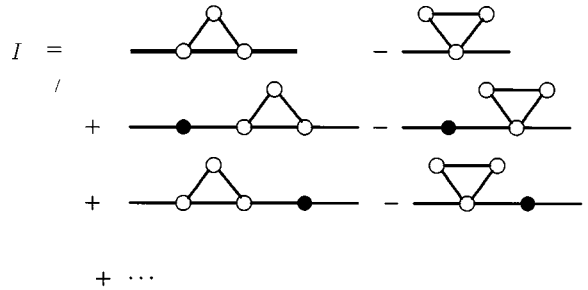

FIG. 1. Diagrams contributing to the irreducible kernal I. Everey full dot symbolizes a potential $V(\rho_i,\rho_j)$: the empty dot represents the structural factor η. A full line is associated with a factor $\delta(\rho_i-\rho_j)/s$. The triangle denotes the three-point function Γ. Furthermore, integrations over all intermediate arguments are implied.

ration average we assume the sites to be statistically independently and uniformly distributed in space. The distribution of site energies is assumed to be given by an arbitrary probability density $p(\{\epsilon\})$. In particular, the application of the averaging procedure to the structural factor η serves as a definition for the density of states, i.e., $\langle\eta(\rho)\rangle=N(\epsilon)$. The process of averaging can be illustrated in the customary way by providing all dots with impurity lines and joining lines. In the course of this operation all diagrams can be decomposed into the irreducible part connected with the function Γ and the reducible remainder. All diagrams giving rise to the remainder can be collected to form the averages of the functions Φ and $\widetilde{\Phi}$, respectively. Consequently, the set of all diagrams contributing to the kernel of the current can be comprised into the form

$$\int d\rho''d\rho'''\widetilde{F}(\rho',\rho'')I_{\rho_1\rho_3\rho_2}(\rho'',\rho''')F(\rho''',\rho), \qquad (20)$$

where $F(\rho',\rho)=\langle\Phi(\rho',\rho)\rangle$, $\widetilde{F}(\rho',\rho)=\langle\widetilde{\Phi}(\rho',\rho)\rangle$, and $I_{\rho_1\rho_3\rho_2}(\rho',\rho)$ is the irreducible part connected with the three-site function Γ. The irreducible part I contains the irreducible parts K and $\widetilde{K}$ originating from the first and the second term of the kernel. A typical diagram that contributes to K is depicted in Fig. 2.

The function F describes the diffusion processes in a four-dimensional $\mathbf{R}-\epsilon$ space.[17] It is a function of the magnitude of the difference of the position vectors, i.e., $F(\rho',\rho)=F(|\mathbf{R}'-\mathbf{R}||\epsilon',\epsilon)$ and satisfies the sum rule[17]

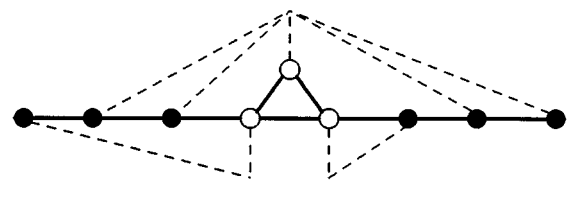

FIG. 2. A typical diagram contributing to the irreducible kernel K. Here every full dot symbolizes a potential $V(\rho_i,\rho_j)$. The empty dot is associated with a structural factor η. The triangle represents the three-point function Γ, a full line the propagator $F(\rho_i,\rho_j)$. The application of the averaging procedure is symbolized by dashed lines. The process of correlated averaging is symbolized by joining lines. Integrations over all intermediate arguments are implied.

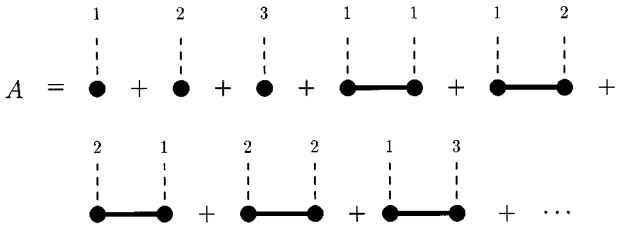

FIG. 3. Diagrams contributing to the the function A. Here every full dot is associated with a factor $C^{-1}(\epsilon')\Gamma(\rho',\widetilde{\rho})\{\delta(\widetilde{\rho}-\rho)-\delta(\rho'-\rho)\}$, where $\rho'(\rho)$ is the argument of the left (right) electron line and $\widetilde{\rho}$ either ρ_1, ρ_2, or ρ_3. The triangle denotes the three point function Γ and the full line the diffsuion propagator F.

$$s\int d\rho F(\rho',\rho)=1. \qquad (21)$$

The function $\widetilde{F}$ is related to F by $\widetilde{F}(\rho',\rho)=F(\rho,\rho')$. Using representation (20) and relation (21) the current can be written in the form

$$\mathbf{j}_H=-\frac{e^2}{kT\Omega}\int d\rho' d\rho d\rho_1 d\rho_2 d\rho_3 \mathbf{R}(\mathbf{E}\mathbf{R}')\{K_{\rho_1\rho_3\rho_2}(\rho',\rho) - \widetilde{K}_{\rho_1\rho_3\rho_2}(\rho',\rho)\}. \qquad (22)$$

It is to be mentioned, that in course of relation (6) the part $\widetilde{K}$, which does not change its topology by exchanging ρ_1 and ρ_3, does not contribute to the Hall current.

The main property of the diagrams contributing to the irreducible part is the fact that points ρ_1, ρ_2, and ρ_3 differ from each other. Due to that fact, the irreducible part contains at least three points.

Below we restrict the calculation of the current to the consideration of three-point diagrams. This restriction is based on a similar appoximation used in Ref. 17 for the calculation of the two-site contribution of the current. There the calculation has been restricted to the inclusion of ladder diagrams. In the three-site description all full dots of the irreducible blocks K and $\widetilde{K}$ are connected with one of the empty points, which permits a summation of all those diagrams. Within this description the irreducible block K can be represented in the form

$$K_{\rho_1\rho_3\rho_2}(\rho',\rho)=\{\delta(\rho'-\rho_1)+A(\rho_1,\rho')\} \times\Gamma(\rho_1,\rho_3,\rho_2)\{\delta(\rho_2-\rho)+A(\rho_2,\rho)\}, \qquad (23)$$

where $A(\rho',\rho)$ is the contribution of the diagrams depicted in Fig. 3. In this picture every full dot represents a contribution of the form $C^{-1}(\epsilon')\Gamma(\rho',\widetilde{\rho})\{\delta(\widetilde{\rho}-\rho)-\delta(\rho'-\rho)\}$, where ρ' (ρ) is the argument of the left (right) electron line and $\widetilde{\rho}$ is either ρ_1, ρ_2, or ρ_3. The full line represents the diffusion propagator F introduced above. The irreducible part $\widetilde{K}$ exhibits a similar representation.

The summation of all contributions is rendered more difficult by the fact that, owing to the function F, the arguments

of consecutive points differ from each other. However, the calculation can be considerably simplified by using the effective-medium approximation proposed in Ref. 17. In this approximation the propagator $F(\rho',\rho)$ is replaced by $fC(\epsilon')\delta(\rho'-\rho)$, where f is a constant that was determined self-consistently in Ref. 17 (see below). In the course of this operation every full dot is replaced by $f\Gamma(\rho',\tilde{\rho})\{\delta(\tilde{\rho}-\rho)-\delta(\rho'-\rho)\}$ and every solid line by $\delta(\rho'-\rho)$.

Inserting Eq. (23) into Eq. (22) we see that the consideration of the function $A(\rho',\rho)$ can be restricted to the quantities $A(\rho_1,\rho)$ and $A(\rho_2,\rho)$. To calculate these quantities in the effective-medium approximation we introduce the function $A^{(i)}(\rho',\rho)$. The function $A^{(i)}(\rho',\rho)$ consists of the subset of diagrams of Fig. 3 that starts with the point $\tilde{\rho}=\rho_i$ ($i=1,2,3$). Using $A^{(i)}$ the quantity A can be written in the form

$$A(\rho',\rho)=\sum_{i=1}^{3} A^{(i)}(\rho',\rho). \tag{24}$$

The functions $A^{(i)}$ satisfy the following system of equations:

$$A^{(i)}(\rho',\rho)=f\Gamma(\rho',\rho_i)\{\delta(\rho_i-\rho)-\delta(\rho'-\rho)\} + f\Gamma(\rho',\rho_i)\{A(\rho_i,\rho)-A(\rho',\rho)\}. \tag{25}$$

For the calculation of the current only a calculation of the nine quantities $A^{(i)}(\rho_j,\rho)$ is needed. As these quantities are antisymmetric with respect to exchanging i and j only three of them are independent. Solving Eq. (25) for those we obtain

$$DA(\rho_1,\rho)=a_{123}\delta(\rho-\rho_2)+a_{132}\delta(\rho-\rho_3) -(a_{123}+a_{132})\delta(\rho-\rho_1), \tag{26}$$

$$a_{123}=f\Gamma_{12}+f^2(\Gamma_{12}\Gamma_{13}+\Gamma_{12}\Gamma_{23}+\Gamma_{13}\Gamma_{23}), \tag{27}$$

$$D=1+2f(\Gamma_{12}+\Gamma_{13}+\Gamma_{23}) +3f^2(\Gamma_{12}\Gamma_{13}+\Gamma_{12}\Gamma_{23}+\Gamma_{13}\Gamma_{23}), \tag{28}$$

where $\Gamma_{ij}=\Gamma(\rho_i,\rho_j)=\Gamma_{ji}$. The quantity $A(\rho_2,\rho)$ can be obtained from Eqs. (26)–(28) by exchanging 1 and 2.

Using the quantities $A(\rho_1,\rho)$ and $A(\rho_2,\rho)$ we obtain an expression for the current. This expression can be further decomposed into its symmetric and antisymmetric parts with respect to the external magnetic field, which describe the magnetoconductivity and the Hall effect, respectively. Using Eq. (5) the symmetric part can be written in the form

$$\mathbf{j}_H^{(s)}=\frac{e^2}{2kT\Omega}\int d\rho_1 d\rho_2 d\rho_3 N(\epsilon_1)N(\epsilon_2)N(\epsilon_3)\Gamma^{(s)}(\rho_1,\rho_3,\rho_2) \times D^{-2}(\rho_1,\rho_2,\rho_3)(\mathbf{R}_{13}b_{123}-\mathbf{R}_{23}b_{213}) \times\{\mathbf{E}(\mathbf{R}_{13}b_{123}-\mathbf{R}_{23}b_{213})\}, \tag{29}$$

where $\mathbf{R}_{ij}=\mathbf{R}_i-\mathbf{R}_j$ and $b_{123}=1+2f\Gamma_{23}+f\Gamma_{13}$. The expression in Ref. 2 differs from those found in the literature (see e.g., Refs. 26–29) in that the statistical correlation between the three sites in question has been taken into account. In derving Eq. (29) all three sites have entered the averaging procedure on equal footing. Moreover, it contains both the processes of energy diffusion and the Fermi correlation, which were neglected in Refs. 27–29.

For the antisymmetric part we obtain

$$\mathbf{j}_H^{(a)}=\frac{e^2}{6kT\Omega}\int d\rho_1 d\rho_2 d\rho_3 N(\epsilon_1)N(\epsilon_2)N(\epsilon_3)\Gamma^{(a)}(\rho_1,\rho_3,\rho_2) \times D^{-2}(\rho_1,\rho_2,\rho_3)(\mathbf{R}_{23}b_{213}-\mathbf{R}_{13}b_{123}) \times\{\mathbf{E}(\mathbf{R}_{13}c_{123}+\mathbf{R}_{23}c_{213})\}, \tag{30}$$

where $c_{123}=1+2f\Gamma_{23}+2f\Gamma_{12}-f\Gamma_{13}$.

IV. HALL EFFECT

The Hall contribution to the current is given by Eq. (30). A further elaboration of its temperature and frequency dependence requires, obviously, the performance of the integrations and the usage of additional theoretical concepts for the density of states. A first step in this direction is the performance of the angular integrations. These integrations can be carried out exactly and yield

$$\mathbf{j}_H^{(a)}=\frac{e^3}{kT\hbar c}\frac{8\pi^2}{9}[\mathbf{E}\times\mathbf{H}] \times\int_0^\infty dR_1 dR_2 \times\int_{|R_1-R_2|}^{R_1+R_2} dR_3 R_1 R_2 R_3 S^2(R_i)g(h(R_i)) \times\int_{-\infty}^{\infty} d\epsilon_1 d\epsilon_2 d\epsilon_3 N(\epsilon_1)N(\epsilon_2)N(\epsilon_3) \times D^{-1}(R_i,\epsilon_i)\Delta(R_i,\epsilon_i). \tag{31}$$

Here we have introduced the function

$$g(h)=\frac{3}{h^2}\left(\frac{\sin(h)}{h}-\cos(h)\right). \tag{32}$$

The parameter h equals the number of flux quanta passing the area S of the triangle formed by the sites R_1, R_2, and R_3. It is given by $h=(eHS)/(\hbar c)$. The function $g(h)$ is introduced in such a way that it approaches 1 for $h\to 0$. Consequently, it can be omitted in the consideration of the linear contribution to the Hall effect with respect to **H**. The function Δ entering Eq. (31) is related to the three-point function $\Gamma^{(a)}$. It is determined by the function Δ' defined by

$$\Gamma^{(a)}(\rho_1,\rho_2,\rho_3)=\Delta'(\rho_1,\rho_2,\rho_3)\sin\{e\mathbf{H}[\mathbf{R}_{13}\times\mathbf{R}_{23}]/(2\hbar c)\}. \tag{33}$$

As Δ' is solely a function of the energies and of the magnitudes of the vectors $\mathbf{R}_{13}$, $\mathbf{R}_{23}$, and $\mathbf{R}_{13}-\mathbf{R}_{23}$, it has the form $\Delta'(\rho_1,\rho_2,\rho_3)=\Delta'(R_{13},R_{23},|\mathbf{R}_{13}-\mathbf{R}_{23}||\epsilon_1,\epsilon_2,\epsilon_3)$. The function Δ is related to Δ' by $\Delta(R_i,\epsilon_i)=\Delta'(R_1,R_2,R_3|\epsilon_1,\epsilon_2,\epsilon_3)$. The details of the calculations leading to Eq. (33) are presented in the Appendix.

Equation (31) describes the Hall effect in the NNH regime, in the VRH regime, and in the region of crossover between them. A further investigation of the Hall contribu-

tion to the current in the region of crossover requires the usage of a concrete model for the density of states in this region and the performance of additional numerical calculations. Below we restrict the consideration to the calculation of the Hall contribution in the NNH and VRH regimes.

A. The Hall effect in the NNH regime

In the NNH regime the transitions occur on the maximum of the density of states. Accordingly, $N(\epsilon)$ can be approximated by $N(\epsilon)=n\delta(\epsilon)$, where n is the concentration of sites at the maximum of the density of states. In the course of this approximation the current reads

$$\mathbf{j}_H^{(a)}=\frac{e^3n^3}{kT\hbar c}\frac{8\pi^2}{9}[\mathbf{E}\times\mathbf{H}]\int_0^\infty dR_1dR_2 \times\int_{|R_1-R_2|}^{R_1+R_2}dR_3R_1R_2R_3S^2(R_i) \times g(h(R_i))D^{-1}(R_i)\Delta(R_i). \tag{34}$$

The quantity Δ is given by $\Delta(R_i)=\nu_3^{(a)}\exp\{-\alpha(R_1+R_2+R_3)\}$. The two site contributions entering D [Eq. (28)] have the form

$$\Gamma_{12}=\nu\exp(-2\alpha R_3), \tag{35}$$

$$\Gamma_{13}=\nu\exp(-2\alpha R_1), \tag{36}$$

where α^{-1} is the localization length of the state. The quantity Γ_{23} is obtained from Eq. (36) by exchanging 1 and 2. The preexponential factors ν and $\nu_3^{(a)}$ depend on the electron-phonon coupling strength.[30] For strong coupling with phonons they are given by

$$\nu=\frac{\sqrt{\pi}}{8\hbar}\frac{J_0^2}{\sqrt{E_akT}}\cosh^{-2}\left(\frac{\epsilon_F}{2kT}\right)\exp\left(-\frac{E_a}{kT}\right), \tag{37}$$

$$\nu_3^{(a)}=\frac{\pi}{8\sqrt{3}}\frac{J_0^3}{\hbar E_akT}\cosh^{-2}\left(\frac{\epsilon_F}{2kT}\right)\exp\left(-\frac{4}{3}\frac{E_a}{kT}\right), \tag{38}$$

where E_a is the activation energy for a small polaron hop and J_0 is the preexponential factor of the resonance integral $[J(R)=J_0\exp(-\alpha R)]$. In the weak-coupling limit the preexponential factors take the form

$$\nu=\tfrac{1}{4}\nu_{\rm ph}\cosh^{-2}\left(\frac{\epsilon_F}{2kT}\right), \tag{39}$$

$$\nu_3^{(a)}=\frac{3}{16}\frac{\hbar\nu_{\rm ph}^2}{J_0}\cosh^{-2}\left(\frac{\epsilon_F}{2kT}\right), \tag{40}$$

where $\nu_{\rm ph}$ is a constant of the order of the characteristic phonon frequency.

For NNH the parameter f has been determined in Ref. 31. It is given by

$$f\nu=\exp(\rho_c) \tag{41}$$

with $\rho_c=2\alpha R_c$, where R_c is the critical hopping length. In the static case we have $R_c=\lambda n^{-1/3}$. The parameter λ is approximately 0.89. The value, which was determined by means of the effective-medium theory, is in good agreement with the percolative results.[30]

In order to perform the residual integrations in Eq. (34) approximately we change the integration variables from R_i to x_i according to $x_i=\alpha R_i-\rho_c/2$. Thereafter, we calculate the integral in the asymtotic limit $\rho_c\to\infty$. The leading contribution to the current reads

$$\mathbf{j}_H^{(a)}=\frac{e^3n^3}{kT\hbar c}\frac{8\pi^2}{9}\kappa\nu_3^{(a)}\alpha^{-10}[\mathbf{E}\times\mathbf{H}] \times\exp(-\tfrac{3}{2}\rho_c)S_c^2g(h_c)\left(\frac{\rho_c}{2}\right)^3. \tag{42}$$

The numerical constant κ is given by

$$\kappa=\int_0^\infty\frac{dy_1dy_2dy_3}{1+2(y_1^2+y_2^2+y_3^2)+3(y_1^2y_2^2+y_1^2y_3^2+y_2^2y_3^2)} =0.291\pi^3. \tag{43}$$

The quantity S_c, given by $S_c=\sqrt{3}R_c^2/4$, represents the dimensionless area of the equilateral triangle with site length R_c, which yields the main contribution to the Hall current. The parameter

$$h_c=\frac{eHS_c}{\hbar c\alpha^2} \tag{44}$$

determines the corresponding number of flux quanta passing the critical triangle. It is to be mentioned, that the validity of Eq. (42) is restricted to magnetic fields obeying $h_c\ll\rho_c$. Using Eq. (42) the Hall conductivity reads

$$\sigma_{xy}=\sin\xi\frac{H}{c}\frac{e^3n^3}{\hbar kT}\frac{\pi^2}{6}\kappa\nu_3^{(a)}\alpha^{-3}R_c^7g(h_c)\exp(-3\alpha R_c). \tag{45}$$

Here ξ is the angle between the direction of the magnetic field and the direction of the electric field.

The Hall mobility is determined by the relation $u_H=(c\sigma_{xy})/(H\sigma_{xx})$. The diagonal component has been calculated in Ref. 31. It is given by

$$\sigma_{xx}=\frac{2\pi}{15}\frac{e^2n^2}{kT}R_c^5\nu\exp(-2\alpha R_c). \tag{46}$$

Accordingly, the Hall mobility takes the form

$$u_H=\frac{5\pi\kappa}{4}\frac{enR_c^2}{\hbar\alpha^3}\frac{\nu_3^{(a)}}{\nu}g(h_c)\exp(-\alpha R_c). \tag{47}$$

Here we have fixed ξ to $\xi=\pi/2$. It is to be mentioned that the fraction involving the preexponential factors depends neither for strong coupling nor for weak coupling with phonons [Eq. (47)] on the position of the Fermi level. Accordingly, Eq. (47) is completely independent of the Fermi level. The fact that the sign of the Hall effect does not change by changing ϵ_F to $-\epsilon_F$ (by changing from electrons to holes) was first observed in Ref. 32 and termed the p-n anomaly of the hopping Hall effect.

In Ref. 3 the Hall effect in the NNH regime has been studied in the linear approximation with respect to the exter-

nal magnetic field by means of percolation theory. The expressions obtained in that paper coincide with our equations in the limit $g(h_c)\to 1$ up to preexponential numerical factors. In Ref. 3 the preexponential factor of σ_{xy} is determined by the correlation length. Referring to this result, the effective-medium method is comparable to the percolation theory in that it leads, like any other self-consistent-field method, to a determination of expressions for the critical index of correlation length. Similar results for the Hall mobility in the NNH regime were also obtained in Refs. 4–8.

According to Refs. 3–6 the main contributions to the current in the NNH regime are governed by configurations of equilateral triangles with side length of the order of the critical hopping length. In a strong magnetic field this fact leads to oscillations of the Hall mobility that depend of the number of flux quanta passing the critical triangle. The disapearance of those oscillations with increasing magnetic field, described by Eq. (32), is related to the rotation of the triangle through the axis of the magnic field that was performed in course of the averaging procedure. Consequently, it does not occur in two-dimensional systems.

B. The Hall effect in the VRH regime

Characteristic for the VRH regime is the fact that the transitions happen near the Fermi surface. Accordingly, as long as the density of states has no pecularities within this region it can be approximated by $N(\epsilon)=N_F$. Introducing the dimensionless variables $r_i=\alpha R_i$ and $z_i=(\epsilon_i-\epsilon_F)/2kT$ expression (31) for the current reads

$$\mathbf{j}_H^{(a)}=\frac{e^3}{\hbar c}\,\frac{16\pi^2}{9}[\mathbf{E}\times\mathbf{H}]N_F^3\alpha^{-10}(2kT)^2G, \tag{48}$$

where

$$G=\int_{-\infty}^{\infty}dz_1dz_2dz_3\int_0^{\infty}dr_1dr_2 \times\int_{|r_1-r_2|}^{r_1+r_2}dr_3\beta(r_i)D^{-1}(r_i,z_i)\Delta(r_i,z_i), \tag{49}$$

$$\beta(r_i)=r_1r_2r_3S^2(r_i)g(h(r_i)). \tag{50}$$

As the functions Γ_{ij} and $\Delta(r_i,z_i)$ differ for strong coupling and weak coupling with phonons we treat these cases seperatly.

1. Strong coupling with phonons

In the strong-coupling limit the quantities Γ_{ij} are given by [compare to Eqs. (35) and (37)]

$$\Gamma_{12}=\nu\,\exp(-2r_3-|z_1|-|z_2|), \tag{51}$$

$$\Gamma_{13}=\nu\,\exp(-2r_2-|z_3|-|z_1|), \tag{52}$$

where

$$\nu=\frac{\sqrt{\pi}}{2\hbar}\,\frac{J_0^2}{\sqrt{E_akT}}\exp\left(-\frac{E_a}{kT}\right). \tag{53}$$

Similarly to the NNH regime the quantity Γ_{23} is obtained from Eq. (53) by replacing 1 by 2. The function Δ has the form [compare to Eq. (38)]

$$\Delta(r_i,z_i)=\nu_3^{(a)}\,\exp(-r_1-r_2-r_3-|z_1|-|z_2|-|z_3| +\tfrac{1}{3}|z_1+z_2+z_3|), \tag{54}$$

where

$$\nu_3^{(a)}=\frac{\pi}{2\sqrt{3}}\,\frac{J_0^3}{\hbar E_akT}\exp\left(-\frac{4}{3}\,\frac{E_a}{kT}\right). \tag{55}$$

The self-consistent parameter f was determined in Ref. 17. It is given by Eq. (41), with $\rho_c=(T_0/T)^{1/4}$, where $T_0=2A(2\alpha)^3/(kN_F)$. The numerical constant A has not been determined so far. Its calculation requires the solution of the diffusion equation in the presence of inelastic scattering.[17]

The quantity G gives rise to two kinds of contributions to the current. The first kind of contributions is determined by configurations that have all energies on the same site of the Fermi surface, the second kind by configurations with energies on different sites of the Fermi surface. However, it turns out that the second group of contributions, which originates from jumps across the Fermi surface, is exponentially small as compared to the first group. Their ratio proves to be of order $\exp(-\rho_c/3)$. Owing to that fact, we restrict our consideration to those configurations having either $z_1,z_2,z_3>0$ or $z_1,z_2,z_3<0$. To calculate G in this approximation we change the variables of the energy integrations to $z_1'=z_1+r_1-r_2+r_3-\rho_c/2$, $z_2'=z_2-r_1+r_2+r_3-\rho_c/2$, $z_3'=z_3+r_1+r_2-r_3-\rho_c/2$. Thereafter, G reads

$$\begin{aligned}G=2\nu_3^{(a)}\,\exp(-\rho_c)&\int_0^{\infty}dr_1dr_2\int_{|r_1-r_2|}^{r_1+r_2}dr_3\beta(r_i)\\ &\times\int_{[r_1-r_2+r_3-(1/2)\,\rho_c]}^{\infty}dz_1'\int_{[r_2-r_1+r_3-(1/2)\,\rho_c]}^{\infty}dz_2'\\ &\times\int_{[r_1+r_2-r_3-(1/2)\,\rho_c]}^{\infty}dz_3'\exp\{-\tfrac{1}{3}(r_1+r_2+r_3)\\ &-\tfrac{2}{3}(z_1'+z_2'+z_3')\}D^{-1}(z_1'+z_2',z_1'+z_3',z_2'+z_3').\end{aligned} \tag{56}$$

Here the arguments of the function D are the arguments of the quantities Γ_{ij} entering D. As the main contributions to the integral arise from the region of small r_i the limit $\rho_c\to\infty$ can be taken easily. Replacing the lower limits of the energy integrations by $-\infty$ we obtain

$$\begin{aligned}G=2\nu_3^{(a)}\kappa'\,\exp(-\rho_c)&\int_0^{\infty}dr_1dr_2\int_{|r_1-r_2|}^{r_1+r_2}dr_3\beta(r_i)\\ &\times\exp\{-\tfrac{1}{3}(r_1+r_2+r_3)\},\end{aligned} \tag{57}$$

where

$$\kappa'=\frac{27}{2}\int_0^{\infty}\frac{dx_1dx_2dx_3}{1+2(x_1^3+x_2^3+x_3^3)+3(x_1^3x_2^3+x_1^3x_3^3+x_2^3x_3^3)}. \tag{58}$$

While the main contributions to the spatial integrations originate from $r_i \sim 1$, the main contributions to the energy integrations arise from the region $0 \leqslant z_i \leqslant \rho_c/2$. Therefore, the most important contributions to the current are determined by configurations forming equilateral triangles with side lengths of order $R_i \approx \alpha^{-1}$ and site energies ranging from 0 to $kT(T_0/T)^{1/4}$ on the same side of the Fermi surface. This fact differs drastically from the situation in the NNH regime, where the most important contributions to the current originate from triangles with side lengths of order R_c.

Owing to the smallness of the typical site length the dimensionless parameter h_c is much smaller in the situation under consideration than in the NNH regime. In fact, it is of order $h_c \approx eH/(\hbar c \alpha^2)$. Therefore, in contrast to the situation in the NNH regime, the linear approximation to current with respect to the magnetic field is applicable even for large magnetic fields. The oscillations of the Hall mobility are absent in the situation under consideration. For practical unattainable large magnetic fields the Hall mobility approaches zero.

Below we restrict the consideration to $h_c \ll 1$. Doing so, we replace $g(h)$ by 1. Performing the integrations we obtain

$$G = \frac{11}{8}\, 3^{12} \nu_3^{(a)} \kappa' \exp(-\rho_c). \tag{59}$$

Therefore, the Hall conductivity takes the form ($\mathbf{H} \perp \mathbf{E}$)

$$\sigma_{xy} = \frac{H}{c}\, 88\pi^2 \kappa' \frac{e^3}{\hbar}\, \nu_3^{(a)} N_F^3 (kT)^2 \left(\frac{3}{\alpha}\right)^{10} \exp\left[-\left(\frac{T_0}{T}\right)^{1/4}\right]. \tag{60}$$

The diagonal contribution to the conductivity σ_{xx} has been investigated in Ref. 17. It is given by

$$\sigma_{xx} = \frac{\pi a}{1260}\, \frac{e^2 \nu N_F^2 kT}{\alpha^5} \left(\frac{T_0}{T}\right)^{7/4} \exp\left[-\left(\frac{T_0}{T}\right)^{1/4}\right], \tag{61}$$

where a equals 4 for strong coupling and 3/2 for weak coupling with phonons. Using Eq. (61) and Eq. (60) the Hall mobility is given by

$$u_H = \frac{1155\pi\kappa' A}{16}\, \frac{e}{\hbar \alpha^2}\, \frac{\nu_3^{(a)}}{\nu} \left(6^4 \frac{T}{T_0}\right)^{11/4}. \tag{62}$$

2. Weak coupling with phonons

In the weak-coupling regime the quantities Γ_{ij} are given by

$$\Gamma_{12} = \nu \exp(-2r_3 - |z_1| - |z_2| - |z_1 - z_2|),$$

$$\Gamma_{13} = \nu \exp(-2r_2 - |z_1| - |z_3| - |z_1 - z_3|), \tag{63}$$

where $\nu = \nu_{\rm ph}$. The quantity Γ_{23} can be obtained from Γ_{13} by changing 1 to 2. The function Δ has the form

$$\Delta(r_i, z_i) = \nu_3^{(a)} \exp(-r_1 - r_2 - r_3)\{[\exp(-|z_1| - |z_2| - |z_1 - z_3| - |z_2 - z_3|)] + [2 \leftrightarrow 3] + [1 \leftrightarrow 3]\}. \tag{64}$$

The preexponential factor is given by $\nu_3^{(a)} = 3\hbar \nu_{\rm ph}^2 / J_0$. The contribution of those configurations that have all energies on the same side of the Fermi surface has the form (there are 12 configurations that can be obtained by exchanging the energies z_i)

$$G = 3\nu_3^{(a)} \int_0^\infty dr_1 dr_2 dr_3 \int_0^\infty dz_3 \int_0^{z_3} dz_2 \int_0^{z_2} dz_1 \times \beta\left(\frac{r_1 + r_2}{2}, \frac{r_1 + r_3}{2}, \frac{r_2 + r_3}{2}\right) \exp(-r_1 - r_2 - r_3 - 2z_3) \times [2 + \exp(2z_1 - 2z_2)] \times D^{-1}(r_1 + r_2 + 2z_2, r_1 + r_3 + 2z_3, r_2 + r_3 + 2z_3). \tag{65}$$

Here the arguments of the function D coincide with the arguments of the functions Γ_{ij} entering D. In order to obtain Eq. (65) we have used the relation

$$\int_0^\infty dr_1 dr_2 \int_{|r_1 - r_2|}^{r_1 + r_2} dr_3 F(r_1, r_2, r_3) = \frac{1}{4} \int_0^\infty dr_1 dr_2 dr_3 F\left(\frac{r_1 + r_2}{2}, \frac{r_1 + r_3}{2}, \frac{r_2 + r_3}{2}\right) \tag{66}$$

that applies to functions that are symmetric with respect to their arguments. In order to calculate the integrals in Eq. (65) we change the variables from z_2 and z_3 to $z_2' = z_2 - \rho_c/2$ and $z_3' = z_3 - \rho_c/2$. Thereafter, we take the limit $\rho_c \to \infty$, so that we obtain

$$G = \frac{3}{4} I \rho_c \exp(-\rho_c), \tag{67}$$

with

$$I = \int_0^\infty dr_1 dr_2 dr_3 \int_{-\infty}^\infty dz_3 \int_0^\infty dz_2 \beta\left(\frac{r_1 + r_2}{2}, \frac{r_1 + r_3}{2}, \frac{r_2 + r_3}{2}\right) \times \exp(-r_1 - r_2 - r_3 - z_3) \times D^{-1}(r_1 + r_2 + z_3 - z_2 + \rho_c, r_1 + r_3 + z_3 + \rho_c, r_2 + r_3 + z_3 + \rho_c). \tag{68}$$

The quantity I depends on the strength of the magnetic field but not on ρ_c. For small magnetic fields it reduces to a numerical coefficient. Similarly to the strong-coupling case the main contributions to integral (65) originate from equilateral triangles with $R_i \sim \alpha^{-1}$. The characteristic energies of two sites are of order $kT(T_0/T)^{1/4}$; the characteristic energy of the third site ranges from 0 to $kT(T_0/T)^{1/4}$.

A further investigation of contributions originating from configurations with site energies on different sides of the Fermi surface reveals that, amongst them, those configurations prove to be most important that are characterized by equilateral triangles of small side length and that have two energies of order $kT(T_0/T)^{1/4}$ on the same side of the Fermi surface and the third energy of order $2kT$ on the other side. Although these contributions are also proportional to $\exp(-\rho_c)$ they are small with respect to the parameter ρ_c^{-1} as compared to the contributions considered above in detail. Therefore, they are omitted in the following. Using Eq. (67) the Hall conductivity takes the form

$$\sigma_{xy}=\frac{H}{c}\frac{16\pi^2}{3}I\frac{e^3}{\hbar}\nu_3^{(a)}\alpha^{-10}N_F^3(kT)^2\left(\frac{T_0}{T}\right)^{1/4}\exp\left[-\left(\frac{T_0}{T}\right)^{1/4}\right]. \tag{69}$$

Consequently, the Hall mobility is given by

$$u_H=70\pi AI\frac{e}{\hbar\alpha^2}\frac{\nu_3^{(a)}}{\nu}\left(16\frac{T}{T_0}\right)^{5/2}. \tag{70}$$

According to our results, the Hall mobility exhibits a powerlike dependence on temperature in the VRH regime in the limit of large ρ_c both for strong coupling and for weak coupling with phonons. In the literature the temperature dependence of the Hall mobility in the VRH regime has been a matter of issue so far. The main point of controversy is related to the presence or absence of an exponentially dependence of the mobility. If we write this dependence in the form

$$u_H\sim\exp\left[-\chi\left(\frac{T_0}{T}\right)^{1/4}\right], \tag{71}$$

where χ is a numerical coefficient, then χ equals 0 in Ref. 3 and Ref. 5. A further result without exponential dependence is to be found in Ref. 9. On the other hand, in Ref. 10 it was concluded that $\chi=3/8$ while in Ref. 11 $\chi=(3/2)^{3/4}-1\approx0.354$ was obtained. The numerical calculation presented in Ref. 12 leads to $\chi\approx0.36$.

The reasons for these deviations are based on the usage of a formula for the nondiagonal component of the conductivity, which was suggested in Ref. 3 and in our notation has the form

$$\sigma_{xy}\sim\left\langle\frac{\Delta(R_1,R_2,R_3,\epsilon_1,\epsilon_2,\epsilon_3)}{\Gamma_{12}\Gamma_{13}+\Gamma_{12}\Gamma_{23}+\Gamma_{13}\Gamma_{23}}\right\rangle. \tag{72}$$

In the framework of percolation theory the averaging is performed over all connected triads that are smaller than the critical triad. In the NNH regime this requirement amounts to a restriction of the side lengths to lengths that are smaller than the critical hoppping length R_c. Therefore, an exponential dependence of the form $\exp(-\alpha R_c)$ has been obtained in all papers (Refs. 3–6), starting with Ref. 3 (the small difference in Ref. 6 is not of principle character). However, in the VRH regime the situation changes drastically. Here the basic requirement

$$2\alpha|R_{ij}|+\frac{1}{2kT}(|\epsilon_i|+|\epsilon_j|+|\epsilon_i-\epsilon_j|)\leqslant\xi \tag{73}$$

(where ξ is a number) does not fix the maximal permissible magnitudes of the side length of the triangle and the energies seperatly but only the sum of these quantities. As Eq. (72) leads to an expression proportional to $\exp(-\alpha\langle R\rangle)$, where $\langle R\rangle$ is the characteristic side length, its application requires the usage of additional assumptions for the determination of the characteristic side length $\langle R\rangle$ and the corresponding characteristic site energies. The effective medium method presented here is free of this arbitrary choice and leads to an automatical determination of the characteristical configurations. As shown above, in the limit of large ρ_c these configurations are given by equilateral triangles with side lengths of order $\langle R\rangle\sim\alpha^{-1}$ both for strong and for weak coupling with phonons.

V. FREQUENCY DEPENDENCE OF THE HALL EFFECT

The effective-medium method presented so far can also be used for studying the frequency dependence of the conductivity. Within the method the frequency dependence is entirely contained in the parameter f, which is reflected in a frequency dependence of the parameter ρ_c. The frequency dependence of the diagonal part of the conductivity was already investigated in Ref. 17 and in Ref. 31. There it was shown, that for small frequencies the conductivity obeys the equation

$$\frac{\sigma_{xx}(\omega)}{\sigma_{xx}(0)}\ln\frac{\sigma_{xx}(\omega)}{\sigma_{xx}(0)}=i\frac{\omega}{\omega_0}. \tag{74}$$

The characteristic frequency ω_0 is of the order of the critical hopping probability (Refs. 17, 31, and 33). As $\sigma_{xx}(\omega)$ and $\sigma_{xx}(0)$ are related to each other by $\sigma_{xx}(\omega)/\sigma_{xx}(0)=\exp[\rho_c(0)-\rho_c(\omega)]$, Eq. (74) can be cast into the form

$$[\rho_c(0)-\rho_c(\omega)]\exp[\rho_c(0)-\rho_c(\omega)]=i\frac{\omega}{\omega_0}. \tag{75}$$

Equation (74) and Eq. (75) are valid for $\omega<\omega_0\exp[\rho_c(0)]$.

Using Eqs. (45), (60), and (69) the frequency dependence of the Hall conductivity can be written as

$$\sigma_{xy}(\omega)=\sigma_{xy}(0)\left(\frac{\rho_c(\omega)}{\rho_c(0)}\right)^{\tau}\exp\{c[\rho_c(0)-\rho_c(\omega)]\}. \tag{76}$$

For NNH the parameters τ, c, and ρ_c are given by $\tau=7$, $c=3/2$, and $\rho_c(0)=2\alpha R_c$. In the VRH regime the parameters c and $\rho_c(0)$ are 1 and $(T_0/T)^{1/4}$, respectively. In this case the parameter τ equals to 0 for strong coupling and to 1 for weak coupling with phonons.

For $\omega\ll\omega_0$ an iteration of Eq. (75) yields

$$\rho_c(\omega)=\rho_c(0)-i\frac{\omega}{\omega_0}+\left(\frac{\omega}{\omega_0}\right)^2+\cdots. \tag{77}$$

Within this region the expansion of the quantity $\sigma_{xy}(\omega)/\sigma_{xy}(0)$ with respect to the parameter ω/ω_0 agrees with the expansion of $\sigma_{xx}(\omega)/\sigma_{xx}(0)$.[31] For $\omega\gg\omega_0$ Eq. (75) can be solved approximately. Doing so, we obtain

$$\rho_c(0)-\rho_c(\omega)\approx\ln\frac{i\omega/\omega_0}{\ln(i\omega/\omega_0)}. \tag{78}$$

Neglecting small contributions of the form $\rho_c^{-1}(0)\ln\ln(\omega/\omega_0)$ we obtain

$$\frac{\sigma_{xy}(\omega)}{\sigma_{xy}(0)}=\left\{1-\frac{1}{\rho_c(0)}\left(i\frac{\pi}{2}+\ln\frac{\omega}{\omega_0}\right)\right\}^{\tau}\left\{\frac{\omega/\omega_0}{\frac{\pi}{2}-i\ln\frac{\omega}{\omega_0}}\right\}^{c}. \tag{79}$$

Omitting small contributions of the type $\rho_c^{-1}(0)\ln(\omega/\omega_0)$ the real part and imaginary part of the Hall conductivity takes the form

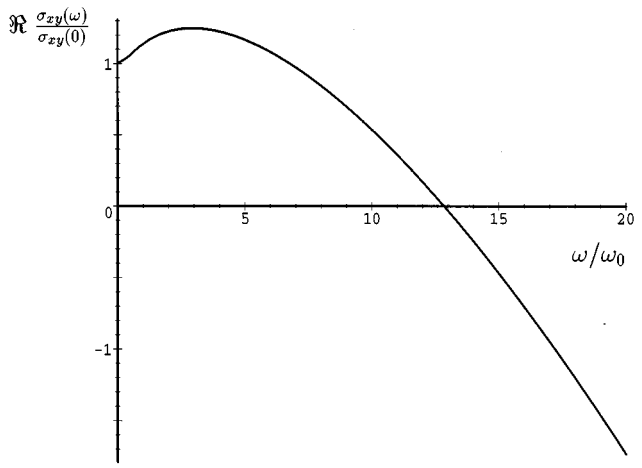

FIG. 4. The real part of the ratio $\sigma_{xy}(\omega)/\sigma_{xy}(0)$ versus ω/ω_0.

$$\mathrm{Re}\,\frac{\sigma_{xy}(\omega)}{\sigma_{xy}(0)}=\frac{\pi}{2}\,\frac{\omega/\omega_0}{\ln^2(\omega/\omega_0)}, \tag{80}$$

$$\mathrm{Im}\,\frac{\sigma_{xy}(\omega)}{\sigma_{xy}(0)}=\frac{\omega/\omega_0}{\ln(\omega/\omega_0)}. \tag{81}$$

Equation (80) and Eq. (81) coincide with the corresponding equations for the diagonal conductivity σ_{xx} in the region under consideration. Consequently, in the VRH regime the Hall mobility depends only weakly on frequency within the considered frequency region. Its dependence is at most of order $\rho_c^{-1}(0)\ln(\omega/\omega_0)$.

The situation changes drastically in the NNH regime. Using Eq. (79) we obtain

$$\mathrm{Re}\,\frac{\sigma_{xy}(\omega)}{\sigma_{xy}(0)}=-\frac{1}{\sqrt{2}}\left(\frac{\omega/\omega_0}{\ln(\omega/\omega_0)}\right)^{3/2}, \tag{82}$$

$$\mathrm{Im}\,\frac{\sigma_{xy}(\omega)}{\sigma_{xy}(0)}=\frac{1}{\sqrt{2}}\left(\frac{\omega/\omega_0}{\ln(\omega/\omega_0)}\right)^{3/2}. \tag{83}$$

According to Eq. (82) the real part of the ratio $\sigma_{xy}(\omega)/\sigma_{xy}(0)$ changes sign (see Fig. 4). This change of sign results in a similar change of sign of the dimensionless frequency-dependent Hall mobility,

$$\frac{u_H(\omega)}{u_H(0)}=\frac{\mathrm{Re}\sigma_{xy}(\omega)/\sigma_{xy}(0)}{\mathrm{Re}\sigma_{xx}(\omega)/\sigma_{xx}(0)}=-\frac{\sqrt{2}}{\pi}\left[\frac{\omega}{\omega_0}\ln\left(\frac{\omega}{\omega_0}\right)\right]^{1/2}. \tag{84}$$

The change of sign, which is strongly related to the difference between the exponents of the static quantities σ_{xy} and σ_{xx}, would also occur in the VRH regime if there was a small exponentially temperature dependence of the static Hall mobility (i.e., if $c>1$ as in Ref. 4, where $c=11/8$).

In the high-frequency limit Eq. (74) and Eq. (75) are inapplicable and the usage of the two-site model for the diagonal component of the conductivty and the three-side model for the nondiagonal part is more appropriate. Within our effective-medium theory this limit is obtained by setting $f=(-i\omega)^{-1}$. The results obtained in this region agree with those obtained in Ref. 1 and Ref. 24. They demonstrate that for high frequencies the Hall mobility depends strongly on frequency. Up to logarithmic contributions its dependence is of the form $u_H(\omega)\sim\omega^{1/2}$.

VI. RESULTS

In this paper we have developed a new effective-medium theory for studying the influence of the magnetic field on hopping transport. The method is based on an effective-medium method that was proposed recently for the calculation of the conductivity in the presence of inelastic scattering.[17] It implies a linearization of the transport equations with respect to the third site that results in expressions for the symmetric and for the antisymmetric part of the configurational averaged current with respect to the external magnetic field, which describe the magnetoconductivity and the Hall effect, respectively. Beside the study of the nonlinear situation with respect to the magnetic field, it permits an investigation of the frequency dependence of the transport coefficients. Furthermore, its range of validity is not restricted to the cases of NNH and VRH but comprises also the whole range of crossover between them.

The method has been applied to the study of the Hall effect both in the NNH regime and in the VRH regime in the presence of static and slowly varying electric fields. Although the analytical tractibility of the integrals is restricted to the percolative limit ($\rho_c\to\infty$) the method proves to be advantegeous. In contrast to other methods, it leads to an automatical determination of the critical configurations that yield the most important contributions to the current. While in the NNH regime the most relevant contributions to the current originate from equilateral triangles with side lenghts of the order of the critical hopping length in the VRH regime for large ρ_c, the most important contributions arise from equilateral triangles with side lengths of the order of the localization length.

The fact that in both regimes the most important contributions originate from different configurations leads to differences between the behavior of the Hall mobility in the NNH regime and its behavior in the VRH regime. In contrast to the NNH regime, where in accordance with Ref. 3 the Hall mobility proves to be exponentially small with respect to the critical hopping length, we obtain a powerlike dependence of the Hall mobility on the critical hopping length in the VRH regime. A similar powerlike dependence has also been obtained in the Refs. 3, 5, and 9 by means of percolation theory. In contrast, the Hall mobility was found to depend exponentially on temperature in Refs. 10 and 11. To this end percolation theory was also applied.

A further consideration of the differences between the various approaches reveals that the discrepancies are caused by different characteristic configurations. Whereas in the present paper and in Refs. 3, 5, and 9 triangles with small areas yield the most important contributions to the Hall current, in Refs. 10 and 11 the most important contributions to the current arise from triangles with side lengths of the order of the critical hopping length. However, in percolation theory there is only one requirement that does not fix the characteristical lengths and energies separately but only the sum. Therefore, within this framework it is hard to decide what the characteristic lengths and energies are. In contrast,

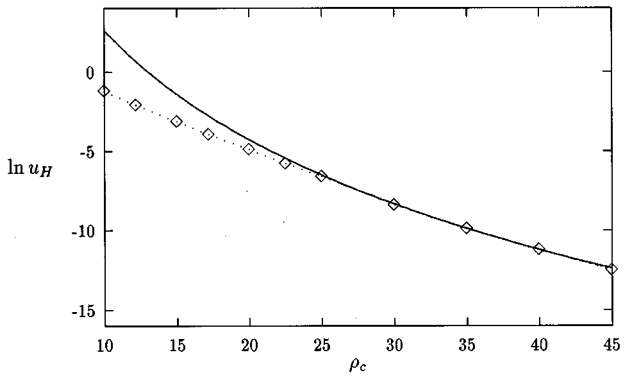

FIG. 5. Logarithm of the Hall mobility versus the critical parameter ρ_c. The dotted line represents the result of the numerical calculations performed in Ref. 12. The solid line displays the result of our effective-medium theory. To achieve correspondence the logarithm of the Hall mobility was represented in the form $\ln u_H = A - 10\rho_c$, where A is a numerical parameter that was determined by means of the data of Ref. 12 for large ρ_c. It is given by $A = 25.6$. For large ρ_c both curves have the same slope.

our formalism leads to an automatical determination of characteristic configurations.

In the experiments reported so far an exponential dependence has also been found (see Refs. 19–21, and 23). However, all these experiments were performed near the metal-insulator transition and within a quite small range of temperatures. In the region under consideration the parameter ρ_c usually ranged between 1 and 4 and the exponential prefactor between 0.3 and 0.5. Within this range the dependence of the Hall mobility is not only determined by the exponential contribution but also by the preexponential factor. Therefore, it is hard to discriminate between a powerlike dependence and an exponential one. The experimental results, which are often represented by means of diagrams showing $\ln \sigma$ in dependence of ρ_c, display often a concave curvature for the Hall conductivity and for the Hall mobility and a convex curvature for the conductivity. Usually this curvature is attributed to a transition from Mott hopping $[\ln \sigma \sim -(T_0/T)^{1/4}]$ to Efros-Shklovskii hopping $[\ln \sigma \sim -(T_0/T)^{1/2}]$. However, such a curvature can also be explained by means of a preexponential powerlike factor.

Owing to the fact that Eqs. (61), (69), and (70) have been derived for $\rho_c \to \infty$ we cannot expect to achieve quantitative agreement with experimental results, but our results are in qualitative agreement with the experimental data. In accordance with the experimental situation the quantities $\ln \sigma_{xy}$ and $\ln u_H$ possess a positive second derivative with respect to ρ_c and the quantity $\ln \sigma_{xx}$ possesses a negative one. However, for large ρ_c ($\rho_c > 25$) they are in good agreement with the numerical results of Ref. 12 (see Fig. 5). A quantitative comparison with the experimental data requires obviously the performance of further numerical calculations of the integrals for ρ_c within the presently experimentally accessible region.

The fact that the characteristic configurations differ in the NNH regime from those in the VRH regime manifest itself also in the frequency dependence of the Hall mobility. In the NNH regime the Hall mobility proves to be strongly dependent on frequency even for low frequencies. For low frequencies [$\omega < \omega_0$, ω_0 charcteristical frequency for NNH (Ref. 31)] the expansion of the Hall conductivity σ_{xy} with respect to the parameter ω/ω_0 parallels the expansion of the conductivity σ_{xx}. For higher frequencies [$\omega_0 < \omega < \omega_0 \exp(\rho_c)$] the exponential dependence of the Hall conductivity results in a change of the sign of its real part. Accordingly, the frequency-dependent dimensionless Hall mobility $\mathrm{Re}[\sigma_{xy}(\omega)/\sigma_{xy}(0)]/\mathrm{Re}[\sigma_{xx}(\omega)/\sigma_{xx}(0)]$ changes its sign too. To our knowledge, this change of sign has not been predicted in the literature so far. It contradicts the results of Ref. 24, where the real part of the Hall conductivity increases monotonously with increasing frequency. For high frequencies our results agree with those found in Ref. 1.

In contrast to the NNH regime, the Hall mobility in the VRH regime is nearly independent of frequency for low and intermediate frequencies. Its frequency dependence reduces to small contributions of the form $\rho_c^{-1} \ln(\omega/\omega_0)$, where ω_0 is a characteristic frequency of the order of the critical hopping probability.[17] For high frequencies our results agree with those found in Ref. 1. It is to be mentioned that a similar change of sign would also occur in the VRH regime if the static Hall mobility exhibited a small exponential temperature dependence, as, for instance, in Ref. 4. Thus, our method provides also a possibility to check our predictions. We emphasize that, even in those cases where the most pronounced temperature dependence is not given by a powerlike dependence on the critical hopping length but the frequency dependence of the longitudinal part of the conductivity is still given by Eq. (74), our method provides experimentalists with a new method of measuring exponential prefactors. Instead of measuring the dc conductivity with varying temperatures we suggest ac measurements with fixed temperature.

Owing to a lack of suitable experimental data it is hard to compare these results to experiments. We are only aware of one experiment where the frequency-dependent Hall effect in the NNH regime was investigated.[2] There the imaginary part of the Hall voltage was measured with fixed frequency ($\omega/\nu_{\mathrm{ph}} \sim 10^{-7}$–$10^{-8}$, $\nu_{\mathrm{ph}} \sim 10^{11}$–$10^{12}\ \mathrm{s}^{-1}$) on doped crystalline Ge and Si samples. The samples were cubes with a side length of 1 cm. The Si sample could be characterized by a wave-function radius of $\alpha^{-1} = 2.2 \times 10^{-7}$ cm and a density of sites of $n = 5 \times 10^{16}\ \mathrm{cm}^{-3}$. The wave-function radius and the site density of the Ge sample were given by $\alpha^{-1} = 7.4 \times 10^{-7}$ cm and $n = 2 \times 10^{15}\ \mathrm{cm}^{-3}$. Voltages of $U = 16$ V and $U = 2.4$ V were applied to the Si sample and to the Ge sample, respectively. The strength of the magnetic field was given by 23 kG. The results were compared with the calculation by Holstein.[1] In contrast to this calculation, which predicted a Hall voltage of 26 μV for the Si sample and a Hall voltage of 270 μV for the Ge sample, the measured Hall voltages proved to be smaller than the noise level of the apparatus, which was estimated to be 2.5 μV for the Si sample and 1.5 μV for the Ge sample. In Ref. 24 it was pointed out that this discrepany is caused by the fact that the experiment was performed in a frequency region, where the two-site approximation has lost its applicability. In our theory the applied frequency belongs to the multiple hopping regime [$\omega_0 < \omega < \omega_0 \exp(\rho_c)$ with $\omega_0 \sim \nu_{\mathrm{ph}} \exp(-\rho_c)$], which is characterized by a strong dependence of both the longitudinal and the transverse part of the conductivity on fre-

quency. Using formulas (82) and (83) we obtain for the imaginary part of the Hall voltage,

$$\mathrm{Im}V_H=\frac{1}{\sqrt{2}}\frac{UH}{c}u_H(0)\left(\frac{\omega/\omega_0}{\ln\omega/\omega_0}\right)^{1/2}. \tag{85}$$

Assuming the magnitude of the resonance integral to be of the order $J_0=0.1$ eV we obtain Hall voltages between $\mathrm{Im}V_H=0.02$ μV and $\mathrm{Im}V_H=0.06$ μV for the Si sample and Hall voltages between $\mathrm{Im}V_H=0.1$ μV and $\mathrm{Im}V_H=0.3$ μV for the Ge sample. Thus, the predictions of our theory are in qualitative agreement with the experimental results of Ref. 2.

The dependence of the Hall effect on the strength of the magnetic field in the VRH regime has been investigated in Refs. 20–23. In these papers the magnetic field ranged between the low-field region and 10 T. A theoretical investigation of the Hall effect in the high-field region requires, besides consideration of the interference factor, also consideration of the wave-function shrinkage. This effect has obviously not been taken into account in our effective-medium theory so far.

In our method the dependence of the Hall conductivity on the magnetic field is governed by the parameter h_c, which equals the number of flux quanta passing the area of critical configuration. As in the VRH regime the most important configurations are given by configurations with small areas the parameter h_c is also small. Consequently, in the VRH regime the linear situation is realized even for large fields. In the NNH regime the parameter h_c is much larger than in the VRH regime. It is given by $h_c=eHn^{-2/3}/\hbar c$. Accordingly, in the presence of large magnetic fields the quantum interferences manifest themselves in quantum oscillations of the Hall conductivity [see Eq. (45)]. The period of these oscillations is given by the normal flux quantum.

ACKNOWLEDGMENTS

This work was supported in part by the Russian Foundation of Fundamental Research under Grant No. 96-02 16848-a.

APPENDIX

Here we perform the integrations leading to Eq. (31). The performance of these integrations proceeds in two steps. At first we analyze the structure of Eq. (30) as well as the effect of the angular integrations on several parts of the integrand further and introduce some simplifications. Thereafter the integrations are carried out explicitly.

In order to simplify Eq. (30) further we mention that in a homogeneous, isotropic space the direction of the Hall contribution to the current should agree with the direction of the pointing vector $\mathbf{S}=[\mathbf{E}\times\mathbf{H}]$. To elaborate on this dependence we rewrite the antisymmetric part of the three-point function Γ in the form

$$\Gamma^{(a)}(\rho_1,\rho_2,\rho_3)=(\mathbf{H}[\mathbf{R}_{13}\times\mathbf{R}_{23}])\,\gamma(\rho_1,\rho_2,\rho_3). \tag{A1}$$

The quantity γ is symmetric with respect to its arguments. Using Eq. (A1) expression (30) for the current reads

$$\mathbf{j}_H^{(a)}=-\frac{e^2}{3kT\Omega}\int d\rho_1 d\rho_2 d\rho_3 N(\epsilon_1) \times N(\epsilon_2)N(\epsilon_3)\gamma(\rho_1,\rho_2,\rho_3)D^{-2}(\rho_1,\rho_2,\rho_3) \times\mathbf{\Psi}(\rho_1,\rho_2,\rho_3), \tag{A2}$$

where

$$\mathbf{\Psi}(\rho_1,\rho_2,\rho_3)=(\mathbf{H}[\mathbf{R}_{13}\times\mathbf{R}_{23}])(\mathbf{R}_{13}b_{123} -\mathbf{R}_{23}b_{213})c_{123}(\mathbf{E}\mathbf{R}_{13}). \tag{A3}$$

Now we consider a rigid triangle formed by the vectors $\mathbf{R}_{13}$ and $\mathbf{R}_{23}$. In order to investigate the effect of averaging over all directions of the triangle with respect to $\mathbf{S}$ we decompose the vector $\mathbf{\Psi}$ into its longitudinal and vertical parts with respect to the pointing vector:

$$\mathbf{\Psi}=\frac{\mathbf{S}(\mathbf{S}\mathbf{\Psi})}{S^2}+\frac{\mathbf{S}\times[\mathbf{S}\times\mathbf{\Psi}]}{S^2}. \tag{A4}$$

After an integration over all directions of the vector Ψ only the first term of Eq. (A4) survives. Consequently, the vector $\mathbf{\Psi}$ in Eq. (32) may be replaced by $\mathbf{S}(\mathbf{S}\mathbf{\Psi})/S^2$. Furthermore, we elaborate on the effect of the angular integrations with respect to the direction of the magnetic field. Decomposing the vectors $\mathbf{R}_{ij}$, entering $\mathbf{\Psi}$ into their longitudinal and vertical parts with respect to the magnetic field, we obtain

$$\mathbf{R}_{ij}=\mathbf{R}_{ij}^{\parallel}+\mathbf{R}_{ij}^{\perp}=\frac{\mathbf{H}(\mathbf{H}\mathbf{R}_{ij})}{H^2}+\frac{\mathbf{H}\times[\mathbf{H}\times\mathbf{R}_{ij}]}{H^2}. \tag{A5}$$

A rotation of $\mathbf{R}_{ij}$ in the vertical plane with respect to $\mathbf{H}$ through π leaves the horizontal part $\mathbf{R}_{ij}^{\parallel}$ unchanged and changes the sign of $\mathbf{R}_{ij}^{\perp}$. As those parts of the integrand that contain $\mathbf{R}_{ij}^{\parallel}$ are odd with respect to $\mathbf{R}_{ij}^{\perp}$ they vanish in the course of the integration. Consequently, the current can be written in the form

$$\mathbf{j}_H^{(a)}=-\frac{e^2}{3kT\Omega}[\mathbf{E}\times\mathbf{H}]\int d\rho_1 d\rho_2 d\rho_3 N(\epsilon_1)N(\epsilon_2)N(\epsilon_3) \times\gamma(\rho_1,\rho_2,\rho_3)D^{-2}(\rho_1,\rho_2,\rho_3)([\boldsymbol{\sigma}\times\mathbf{R}_{13}^{\perp}][\mathbf{R}_{13}^{\perp}\times\mathbf{R}_{23}^{\perp}]) \times c_{123}\{b_{123}(\boldsymbol{\sigma}\mathbf{R}_{13}^{\perp})-b_{213}(\boldsymbol{\sigma}\mathbf{R}_{23}^{\perp})\}, \tag{A6}$$

where $\boldsymbol{\sigma}$ is the unit vector the $\mathbf{S}$ direction. As the vectors $\boldsymbol{\sigma}$, $\mathbf{R}_{13}^{\perp}$, and $\mathbf{R}_{23}^{\perp}$ lie in the same plane perpendicular to the magnetic field, the problem of integrating out the angular dependence has been considerably simplified. In fact, it has been reduced to an integration over the angle enclosed by one site of the rigid triangle and the direction of $\boldsymbol{\sigma}$ and an integration over the triangle encompassed by the sites $\mathbf{R}_{13}^{\perp}$ and $\mathbf{R}_{23}^{\perp}$.

At first we consider the integration over the angel encompassed by the vector $\mathbf{R}_{13}^{\perp}$ and the direction of the pointing vector. In performing this integration the angle between $\mathbf{R}_{13}^{\perp}$ and $\mathbf{R}_{23}^{\perp}$ is kept fixed. In the course of the integrations only the term proportional to b_{213} survives. Its angular-dependent part $([\boldsymbol{\sigma}\times\mathbf{R}_{13}^{\perp}][\mathbf{R}_{13}^{\perp}\times\mathbf{R}_{23}^{\perp}])(\boldsymbol{\sigma}\mathbf{R}_{23}^{\perp})$ is replaced by $1/2[\mathbf{R}_{13}^{\perp}\times\mathbf{R}_{23}^{\perp}]^2$. Using the symmetry of the functions γ and D with respect to their arguments the product $c_{123}b_{213}$ can be replaced by D. Finally, taking into account the fact that all functions depend solely on the differences $\mathbf{R}_{13}$ and $\mathbf{R}_{23}$, the

integration over the third point, being the initial point of the coordinate system, can be performed too. In doing so, we obtain

$$\mathbf{j}_H^{(a)}=\frac{e^2}{6kT}[\mathbf{E}\times\mathbf{H}]\int d\rho_1 d\rho_2 d\epsilon_3 \gamma(\rho_1,\rho_2,\rho_3) \times D^{-1}(\rho_1,\rho_2,\rho_3)N(\epsilon_1)N(\epsilon_2)N(\epsilon_3)[\mathbf{R}_1^{\perp}\times\mathbf{R}_2^{\perp}]^2, \tag{A7}$$

where $\rho_3=(0,\epsilon_3)$. To perform the remaining angular integrations we rewrite γ in the form

$$\gamma(\rho_1,\rho_2,\rho_3)=\Delta'(\rho_1,\rho_2,\rho_3)\,\frac{\sin\{e\mathbf{H}[\mathbf{R}_1\times\mathbf{R}_2]/(2\hbar c)\}}{\mathbf{H}[\mathbf{R}_1\times\mathbf{R}_2]}. \tag{A8}$$

The quantity $\Delta'(\rho_1,\rho_2,\rho_3)$ has already been introduced in Eq. (33). The functions Δ' and D entering expression (A7) depend on the energies ϵ_1, ϵ_2, and ϵ_3 and on the length of the sites of the triangle $|\mathbf{R}_1|$, $|\mathbf{R}_2|$ and $R_3=\sqrt{R_1^2+R_2^2-2R_1R_2\cos\psi}$, where ψ is the angle encompassed by $\mathbf{R}_1$ and $\mathbf{R}_2$. Representing the vectors $\mathbf{R}_1$ and $\mathbf{R}_2$ in spherical coordinates we obtain

$$\cos\psi=\cos(\alpha_1-\alpha_2)\sin\theta_1\sin\theta_2+\cos\theta_1\cos\theta_2, \tag{A9}$$

where θ_1,θ_2 and α_1,α_2 are the polar and azimutal angles, respectively. The direction of the polar axis of the coordinate system agrees with the direction of the magnetic field. The integration over ψ can be simplified by introducing R_3 as an additional integration variable. This is achieved by inserting the identity

$$1=2\int_{|\mathbf{R}_1-\mathbf{R}_2|}^{R_1+R_2} dR_3 R_3\,\delta(R_3^2-R_1^2-R_2^2+2R_1R_2\cos\psi). \tag{A10}$$

Thereafter expression (A7) for the current reads

$$\mathbf{j}_H^{(a)}=\frac{e^2}{3kT}[\mathbf{E}\times\mathbf{H}]\int_0^{\infty} dR_1 dR_2 \int_{|\mathbf{R}_1-\mathbf{R}_2|}^{R_1+R_2} dR_3 \times\int_{-\infty}^{\infty} d\epsilon_1 d\epsilon_2 d\epsilon_3 N(\epsilon_1)N(\epsilon_2)N(\epsilon_3) \times R_1^2R_2^2R_3D^{-1}(R_i,\epsilon_i)\Delta(R_i,\epsilon_i)I(R_i). \tag{A11}$$

The quantity $I(R_i)$ contains the remaining angular integrations. It is given by

$$I(R_i)=\frac{R_1R_2}{H}\int_0^{2\pi} d\alpha_1 d\alpha_2 \int_0^{\pi} d\theta_1 d\theta_2 \sin^2\theta_1\sin^2\theta_2 \times\sin(\alpha_1-\alpha_2)\sin\left\{\frac{eHR_1R_2}{2\hbar c}\sin(\alpha_1-\alpha_2) \times\sin\theta_1\sin\theta_2\right\}\delta(R_3^2-R_1^2-R_2^2+2R_1R_2\cos\psi). \tag{A12}$$

Performing the integrations over α_1 and α_2 we obtain

$$I=\frac{2\pi}{H}\int d\theta_1 d\theta_2 \sin \times[\Phi\sqrt{(\cos\theta_1\cos\theta_2)^2-(y-\sin\theta_1\sin\theta_2)^2}], \tag{A13}$$

where $\Phi=eHR_1R_2/(2\hbar c)$. The range of integration in Eq. (A13) is restricted to the area $-\pi/2\leqslant\theta_1,\theta_2\leqslant$, $(\cos\theta_1\cos\theta_2)^2\geqslant(y-\sin\theta_1\sin\theta_2)^2$, where $y=(R_1^2+R_2^2-R_3^2)/(2R_1R_2)$. The quantity y ranges between $-1\leqslant y\leqslant 1$. Introducing the new coordinates x and ϕ, according to $x\sin\phi=\sin\theta_1$, $x\cos\phi=\sin\theta_2$, expression (A13) takes the form

$$I=\frac{2\pi(1-y^2)}{H}\int_0^1 dx x\,\sin(\Phi x\sqrt{1-y^2}) \times\int_0^{\pi} d\phi\left(\frac{1}{1+y\,\sin\phi}+\frac{1}{1-y\,\sin\phi}\right). \tag{A14}$$

Calculating these integrals we obtain

$$I=\frac{8\pi^2}{3R_1R_2}\frac{eS^2}{\hbar c}g(h). \tag{A15}$$

Inserting Eq. (A15) into Eq. (A11) we obtain Eq. (31).

[1] T. Holstein, Phys. Rev. **124**, 1329 (1961).
[2] M. Amitay and M. Pollak, J. Phys. Soc. Jpn. Suppl. **21**, 549 (1966).
[3] H. Böttger and V. V. Bryksin, Phys. Status Solidi B **81**, 433 (1977).
[4] B. Movaghar, B. Pohlmann, and D. Würtz, J. Phys. C **14**, 5127 (1981).
[5] Yu. M. Gal'perin, E. P. German, and V. G. Karpov, Zh. Eksp. Teor. Fiz. **99**, 343 (1991) [Sov. Phys. JETP **72**, 193 (1991)].
[6] L. Friedman and M. Pollak, Philos. Mag. B **38**, 173 (1978).
[7] B. Movaghar, M. Grünewald, B. Pohlmann, D. Würtz, and W. Schirmacher, J. Stat. Phys. **30**, 315 (1983).
[8] J. A. McInnes and P. N. Butcher, Philos. Mag. B **44**, 595 (1981).
[9] L. Friedman, and M. Pollak, Philos. Mag. B **44**, 487 (1981).
[10] M. Grünewald, H. Müller, P. Thomas, and D. Würtz, Solid State Commun. **38**, 1011 (1981).
[11] R. Ne'meth and B. Mühlschlegel, Solid State Commun. **66**, 999 (1988).
[12] R. Ne'meth, Physica B **167**, 1 (1990).
[13] H. Overhof and P. Thomas, Phys. Rev. B **53**, 13 187 (1996).

[14] O. Bleibaum, H. Böttger, and V. V. Bryksin, Phys. Rev. B **53**, 13 190 (1996).
[15] B. Movaghar and W. Schirmacher, J. Phys. C **14**, 859 (1981).
[16] D. Bourbie, Philos. Mag. B **73**, 201 (1996).
[17] O. Bleibaum, H. Böttger, and V. V. Bryksin, Phys. Rev. B **54**, 5444 (1996).
[18] C. R. Gochanour, H. C. Andersen, and M. D. Fayer, J. Chem. Phys. **70**, 4254 (1979).
[19] D. W. Koon and T. G. Castner, Solid State Commun. **64**, 11 (1987).
[20] A. Roy, M. Levy, X. M. Guo, and M. P. Sarachik, Phys. Rev. B **39**, 10 185 (1989).
[21] Youzhu Zhang, Peihua Dai, Irene Kam, and M. P. Sarachik, Phys. Rev. B **49**, 5032 (1994).
[22] Youzhu Zhang, Peihua Dai, and M. P. Sarachik, Phys. Rev. B **45**, 6301 (1992).
[23] D. W. Koon, and T. G. Castner, Phys. Rev. B **41**, 12 054 (1990).
[24] B. Movaghar, P. Pohlmann, and D. Würtz, J. Phys. C **14**, 5127 (1981).
[25] H. Böttger, V. V. Bryksin, and F. Schulz, Phys. Rev. B **49**, 2447 (1994); **51**, 14 020 (1995).
[26] O. Bleibaum, H. Böttger, V. V. Bryksin, and F. Schulz, Phys. Rev. B **51**, 14 020 (1995).
[27] W. Schirmacher, Phys. Rev. B **41**, 2461 (1990).
[28] W. Schirmacher, H. T. Fritzsche, and R. Kempter, Solid State Commun. **88**, 125 (1993).
[29] H. Fritzsche and W. Schirmacher, Europhys. Lett. **21**, 67 (1993).
[30] H. Böttger and V. V. Bryksin, *Hopping Conduction in Solids* (Akademie-Verlag, Berlin, 1985).
[31] V. V. Bryksin, Fiz. Tverd. Tela (Leningrad) **26**, 1362 (1984) [Sov. Phys. Solid State **26**, 827 (1984)].
[32] T. Holstein, Philos. Mag. **27**, 255 (1973).
[33] V. V. Bryksin, Fiz. Tverd. Tela (Leningrad) **22**, 2441 (1980) [Sov. Phys. Solid State **22**, 2441 (1980)].